Journal of Integrative Neuroscience

J. Integr. Neurosci. **2025**; 24(10): 42821
https://doi.org/10.31083/JIN42821

Original Research

Exploring the Functional Connectivity of Resting-state EEG in Adolescent Major Depressive Disorder

Yanna Kou[1,2,†], Yajing Si[1,3,4,†], Lu Liu[5,6], Juan Li[1], Yan Zhang[1,2], Wenqiang Li[1], Junlei Zhang[1], Chuansheng Wang[1,*], Hongxing Zhang[1,4,7,8,*]

[1]Department of Child and Adolescent Psychiatry, The Second Affiliated Hospital of Xinxiang Medical University, 453000 Xinxiang, Henan, China
[2]Xinxiang Key Laboratory of Child and Adolescent Psychiatry, 453000 Xinxiang, Henan, China
[3]Henan Key Lab of Biological Psychiatry, Xinxiang Medical University, 453000 Xinxiang, Henan, China
[4]School of Psychology, Xinxiang Medical University, 453000 Xinxiang, Henan, China
[5]Peking University Sixth Hospital/Institute of Mental Health, National Clinical Research Center for Mental Disorders (Peking University Sixth Hospital), 100000 Beijing, China
[6]Key Laboratory of Mental Health, Ministry of Health (Peking University), 100191 Beijing, China
[7]The Pediatrics Department of the First Affiliated Hospital of Xinxiang Medical University, 453003 Xinxiang, Henan, China
[8]Xinxiang Key Laboratory of Psychopathology and Cognitive Neuroscience, 453002 Xinxiang, Henan, China
*Correspondence: chuansonwang@126.com (Chuansheng Wang); zhx166666@163.com (Hongxing Zhang)
[†]These authors contributed equally.

Academic Editor: Bettina Platt
Submitted: 2 June 2025 Revised: 21 August 2025 Accepted: 12 September 2025 Published: 30 October 2025

Abstract

Background: This study aimed to explore the potential relationship between resting-state brain network attributes and adolescent major depressive disorder (MDD), with a focus on understanding how resting-state electroencephalogram (EEG) network features correlate with Hamilton Depression Rating Scale (HAMD) scores, and to identify potential physiological biomarkers for predicting HAMD scores in adolescents with MDD. **Methods**: Adolescent MDD presents unique neurodevelopmental challenges, yet the neurophysiological correlates of symptom severity remain poorly characterized. This study investigated resting-state EEG network topology and its relationship with HAMD scores in adolescent MDD, aiming to identify potential neural biomarkers for depression severity. **Results**: MDD patients exhibited significantly enhanced frontal-parietal connectivity compared with healthy controls (HC) ($p < 0.05$, false discovery rate (FDR)-corrected). HAMD scores correlated positively with coefficient (Clu) (r = 0.401), global efficiency (Ge) (r = 0.408), and local efficiency (Le) (r = 0.402), while showing a negative correlation with characteristic path length (Cpl) (r = –0.408; all PFDR < 0.05). The regression model achieved strong prediction accuracy ($R^2 = 0.38$, $p < 0.001$; root mean square error (RMSE) = 2.83), and network features distinguished MDD from HC with 94% classification accuracy. **Conclusion**: These preliminary findings deepen our understanding of adolescents with MDD and suggest that resting-state brain network attributes in the alpha band may serve as a potential physiological biomarker for predicting HAMD scores.

Keywords: major depressive disorder; adolescent; HAMD; resting-state network; EEG

1. Introduction

Major depressive disorder (MDD) is a complex condition characterized by disrupted neural networks and impairments in cognitive and emotional processing, typically marked by persistent low mood, pessimism, heightened sensitivity, and dysregulation of cognitive control [1,2]. Recently, the prevalence of MDD has exhibited a notable shift toward younger populations, affecting up to 20% of adolescents. This early onset poses serious concerns, as it substantially interferes with academic performance, daily functioning, and elevates the risk of suicide [3,4]. While clinical manifestations of adolescent MDD—such as emotional instability, irritability, and heightened sensitivity—are increasingly recognized, the underlying neurobiological mechanisms, particularly those involving aberrant functional connectivity between brain regions, remain inadequately understood [5].

Previous studies based on structural magnetic resonance imaging (MRI) have reported morphological and microstructural changes, such as reductions in gray matter in the prefrontal regions, hippocampal volume, and total cortical surface area [6–8], as well as alterations in the microstructure of white matter fiber bundles [9,10] in the brains of adolescents with MDD. Recent reviews on functional MRI (fMRI) studies of MDD have found that abnormal brain function can lead to changes in the default mode network (DMN) and frontoparietal network (FPN) [6,11–15]. Notably, investigations focusing on the frontoparietal regions in individuals with MDD have revealed significantly elevated levels of both functional and effective connectivity between the parietal and prefrontal cortices during task-related states. Moreover, the strength of this connectivity has been shown to exhibit a positive correlation with depression severity [16,17].

The brain usually operates as a large-scale complex network composed of interconnected regions, transmitting and integrating information between these spatially separated but functionally coupled areas to ensure efficiency in responding to upcoming stimuli [18]. The brain continues to function in a resting state, and its spontaneous neuronal activity may reflect the brain's underlying information-processing capabilities [19]. Particularly, the resting-state network can thus effectively reflect the internal allocation of brain resources. Given the millisecond-level information processing capabilities of the brain, the electroencephalogram (EEG), with its high temporal resolution, has greater advantages over fMRI in analyzing time-varying brain networks [20].

Previous EEG studies on MDD have mainly focused on abnormalities in the emotional face, auditory attention, and feedback [4,15,21,22]. Although emerging evidence indicates that aberrant brain functional connectivity may be present in adolescents with MDD, these alterations appear to be linked with the severity of clinical symptoms [23–25]. The systematic review literature highlights that abnormal alpha band activity in brain oscillations is significantly correlated with depressive symptom severity and serves as a biomarker for cognitive dysfunction in depression [20,26]. Recent studies have suggested that alpha activity has potential significance in assessing the severity of depression as a supplementary diagnostic tool [27,28]. Previous investigations of alpha-band activity in individuals with MDD have predominantly concentrated on metrics such as peak amplitude and frequency. However, the role of underlying functional network topological properties—which are critical for optimizing neural information processing—has received comparatively limited attention [29]. Specifically, while alpha oscillations are acknowledged as neurophysiological markers relevant to cognitive performance, the topological features of the brain's functional framework within this frequency band remain underexplored in the context of MDD [30].

Specifically, indices of brain network topological attributes such as the clustering coefficient (*Clu*), global efficiency (*Ge*), local efficiency (*Le*), and characteristic path length (*Cpl*) can depict the brain network's information integration and segregation capabilities from different perspectives [31]. Notably, abnormalities in these attributes have been observed in adult MDD [32]. However, due to enhanced neuroplasticity in the adolescent brain, its network topology may exhibit unique compensatory or pathological patterns—a direction that has not yet been systematically explored [33]. To bridge this gap, the current study examined the association between resting-state EEG-derived functional brain networks and Hamilton Depression Rating Scale (HAMD) scores. Furthermore, we assessed the feasibility of predicting HAMD scores within the MDD group based on connectivity features extracted from resting-state EEG. These findings may contribute to the identification of potential neurophysiological biomarkers for the diagnosis and clinical evaluation of adolescent MDD.

2. Materials and Methods

2.1 Participants

This study was approved by the Institutional Review Board and Ethics Committee of the Second Affiliated Hospital of Xinxiang Medical University (approval number: XYEFYJSSJ-2023-12), and all participants and their guardians signed a written informed consent form. Our study conformed to the ethical guidelines of the World Medical Association Declaration of Helsinki. Twenty-seven MDD patients were recruited from the outpatient department and inpatient department of the Second Affiliated Hospital of Xinxiang Medical University from October 2023 to May 2024. The inclusion criteria were: (1) A diagnosis of depression that met the diagnostic criteria for MDD in the Kiddie-Schedule for Affective Disorders and Schizophrenia Present and Lifetime Version (K-SADS-PL) and the Diagnostic and Statistical Manual of Mental Disorders, 4th Edition (DSM-IV); (2) no antipsychotic medication treatment within one month before admission; (3) Han ethnicity and right-handed. The exclusion criteria were: (1) Co-occurring craniocerebral trauma, stroke, and other central nervous system diseases; (2) Presence of obvious brain organic lesions; (3) Severe metabolic and endocrine system diseases; (4) Other types of mental disorders as described in K-SADS-PL and DSM-IV.

The MDD group included a total of 10 males and 17 females. During subsequent analysis, two female participants were excluded due to excessive artifacts in resting-state EEG data, resulting in a final selection of 10 males and 15 females. The mean age was (14.24 $\pm$ 1.23) years, ranging from 11 to 18 years; the duration of illness was (10.60 $\pm$ 4.43) months, ranging from 6 to 16 months; the 17-item Hamilton Depression Scale (HAMD-17) score was (24.76 $\pm$ 3.70). Additionally, 26 healthy controls (HC) matched for gender and age with the MDD patients were recruited from a middle school in Xinxiang City during the same period. All members of the HC and their first-degree relatives had no history of mental illness, and the exclusion criteria were the same as for the MDD group. The HC initially included 11 males and 15 females, but due to excessive artifacts in the resting-state EEG data, one male participant was excluded, resulting in a final selection of 10 males and 15 females. The mean age was (13.96 $\pm$ 1.02) years, ranging from 11 to 18 years. There were no statistically significant differences in the gender ratio or age between the two groups ($\chi^2 = 0.87$, $p = 0.390$; $t = 0$, $p = 1$).

2.2 Experimental Procedure

According to the experimental setup, we gathered resting-state EEG data from the participants, which included five minutes of resting with their eyes closed. Ask-

ing a participant to (1) remain relaxed and focused, and (2) refrain from excessive head motion to ensure the validity of the EEG data.

2.3 EEG Acquisition

Using the EEG amplifier from Brain Products along with the data acquisition software, BrainVision 2.0 (Brain Products GmbH, Gilching, Germany), we collected 32-channel resting-state EEG data. The arrangement of the scalp electrodes was based on the internationally standardized 10/20 system. The basic parameters of the amplifier included a sampling frequency of 1000 Hz, and an online band-pass filter scope of 0.01–100 Hz, with the FCz electrode serving as the reference and AFz electrode as the ground. The horizontal electrooculogram (HEOG) was placed below the left eye, and the vertical electrooculogram (VEOG) was placed at the outer corner of the right eye to monitor and record the participants' blink activity. To ensure signal reliability, an appropriate amount of conductive gel was applied to the electrodes to keep the contact impedance between the electrodes and the scalp below 5 kΩ.

2.4 EEG Analysis

The processing of resting-state data aimed to structure the resting-state network and extract related network attribute measures. Below, we describe the analysis process for each section in detail.

2.4.1 Resting-state EEG Brain Network

To mitigate the volume conduction effect, we selected 21 electrodes (Fpz, Fp1, Fp2, Fz, F3, F4, F7, F8, Cz, C3, C4, T7, T8, Pz, P3, P4, P7, P8, Oz, O1, O2) from the 32 electrodes of the 10/20 system that were sparsely distributed and covered the whole brain to makeup the resting-state networks. The preprocessing procedures included reference electrode standardization technique (REST) referencing, 0.5–40 Hz bandpass filtering, segmenting the data into multiple bands (delta: 0.5–4 Hz, theta: 4–8 Hz, alpha: 8–13 Hz, beta: 13–30 Hz, and gamma: 30–45 Hz) by Finite Impulse Response (FIR) filter in Matlab, artifact removal (with a threshold of ±60 μV), and segmenting the data into 5-s epochs. This epoch length was chosen based on previous study [34], which demonstrated that 5-second windows provide a suitable trade-off between temporal resolution and signal stability for alpha-band phase synchronization analysis. After the preprocessing of the EEG data, the ranges of effective segments for the HC and MDD groups were 91 ± 31 and 73 ± 10, respectively. We conducted an independent samples *t*-test to compare the number of clean segments between the MDD and control groups. The results revealed a significant difference: $t = 2.7585$, $p = 0.0082$ ($p < 0.05$), indicating that the MDD group had expressively fewer clean segments compared to the healthy controls. Based on the average number of data segments of the subjects in the MDD group, for each subject in the control group, the number of data segments consistent with the average was randomly selected. Network attributes were calculated using the Brain Connectivity Toolbox [35].

Based on the preprocessed resting-state segments, we construct resting-state brain network by phase locking value (PLV) algorithm. As a nonlinear measure, the PLV can provide information on phase synchronization between different brain regions and calculate the phase synchronization between per pair of electrodes. After constructing the related resting-state networks, let C_{ij} represent the PLV between nodes i and j within the network, d_{ij} represents the weighted shortest path length between nodes i and j, N represents the number of network nodes, and Θ represents the set of all nodes within the network. Using graph theory and the Brain Connectivity Toolbox, we calculated multiple network attributes that quantify the efficiency of brain information processing, containing the clustering coefficient (*Clu*), characteristic path length (*Cpl*), global efficiency (*Ge*), and local efficiency (*Le*).

$$Clu = \frac{1}{N}\sum_{i\in\Theta}\frac{\sum_{j,l\in\Theta}(C_{ij}C_{il}C_{jl})^{1/3}}{\sum_{j\in\Theta}C_{ij}\left(\sum_{j\in\Theta}C_{ij}-1\right)} \tag{1}$$

$$Cpl = \frac{1}{N}\sum_{i\in\Theta}Li = \frac{1}{N}\sum_{i\in\Theta}\frac{\sum_{j\in\Theta,j\neq i}d_{ij}}{N-1} \tag{2}$$

$$Ge = \frac{1}{N}\sum_{i\in\Theta}\frac{\sum_{j\in\Theta,j\neq i}d_{ij}^{-1}}{N-1} \tag{3}$$

$$Le = \frac{1}{N}\sum_{i\in\Theta}\frac{\sum_{j,l\in\Theta,j\neq i}\left(C_{ij}C_{jl}[d_{jl}(\Theta_i)]^{-1}\right)^{1/3}}{\sum_{j\in\Theta}C_{ij}\left(\sum_{j\in\Theta}Cij-1\right)} \tag{4}$$

2.4.2 Prediction of HAMD Scores Grounded on Multivariable Linear Regression Model

Thereafter, we used the resting-state network topologies (network connectivity edges) and attributes (*Clu*, *Le*, *Ge*, and *Cpl*) of adolescent MDD as variables in a multivariable linear regression model to construct a prediction model. The prediction model is as follows:

$$HAMD = \beta_0 + \beta_1 Topo + \beta_2 Prop + \varepsilon \tag{5}$$

where HAMD represents the HAMD scores, $\beta_{0\ldots2}$ indicates the regression coefficients, Topo denotes the network con-

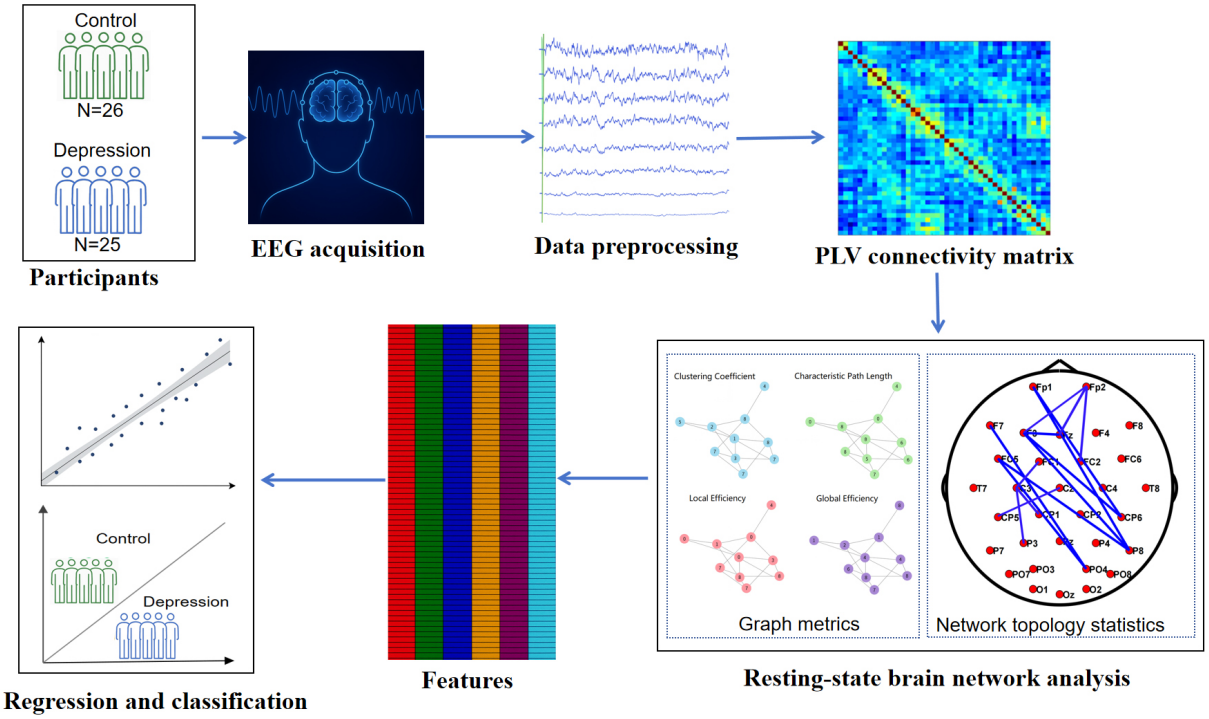

Fig. 1. Overview of the EEG-based resting-state network analysis pipeline for regression and classification of depression. PLV, phase locking value; EEG, electroencephalogram.

nectivity edge, Prop represents the network attributes and $\mathcal{E}$ is the error term.

A leave-one-out cross-validation (LOOCV) strategy was employed to predict HAMD scores [36]. For n samples, in each cross-validation iteration, $n - 1$ samples were used as the training set, and the remaining one sample was used as the test sample. Based on the $n - 1$ samples, the regression coefficients for each variable can be estimated, thereby establishing a prediction model. This model can be used to predict the HAMD scores within the test set. This procedure is repeated n times until all samples have been served as a test sample.

To quantitatively measure the predictive result of this prediction model, the correlation between the actual and divinable HAMD scores was analyzed using Pearson's correlation. Additionally, the prediction error was further measured by the root mean square error (RMSE), which is specifically defined as follows,

$$RMSE = \sqrt{\frac{1}{N}\sum_{t=1}^{N}(X_t - Y_t)^2} \quad (6)$$

where N is the number of samples. X and Y represent the observed and predicted HAMD scores, respectively, and a smaller $RMSE$ represents better prediction.

2.4.3 Classification Based on Network Features

During the training process, the resting-state network characteristics extracted from the training set were used to train the corresponding classifiers. Specifically, for network features, the network features of the resting-state training set were obtained based on a 21 $\times$ 21 adjacency matrix; for network attributes, the resting-state weighted network attributes of the training set were calculated accordingly. Linear discriminant analysis (LDA) was employed as the classifier and was trained with the resting-state multi-type feature sets, resulting in the acquisition of model parameters. During the testing process, for the test set, the resting-state weighted network attributes of the test set were calculated in a manner similar to the training process; finally, grounded on the aforementioned features (i.e., network topology and attributes), the trained LDA classifier was used to diagnose and differentiate adolescent depression patients from healthy controls in the test data.

2.5 Statistical Analysis

Independent sample t-tests were used to evaluate the differences in resting-state EEG network topology between the MDD and HC groups. Within the MDD group, Pearson's correlation was employed to investigate the relationships between HAMD scores and resting-state network edges, as well as network attributes. Furthermore, the false discovery rate (FDR) was applied to correct these results, with a p-value of less than 0.05 considered statistically significant. Fig. 1 shows the pipeline of our method.

Table 1. Baseline characteristics of the MDD and HC groups.

Characteristic	MDD Group (n = 25)	HC Group (n = 25)	*p*
Age (years, mean ± SD)	14.24 ± 1.23	13.96 ± 1.02	0.33
Gender, n (%)			1.00
Male	10 (40%)	10 (40%)	
Female	15 (60%)	15 (60%)	
Illness duration (months)	10.60 ± 4.43	-	-
HAMD scores	24.76 ± 3.70	0	<0.001

Note: MDD, major depressive disorder; HC, healthy controls; SD, standard deviation; HAMD, hamilton depression rating scale. The HAMD score for the HC group is 0 as they had no depressive symptoms, and thus no statistical test was performed for this comparison.

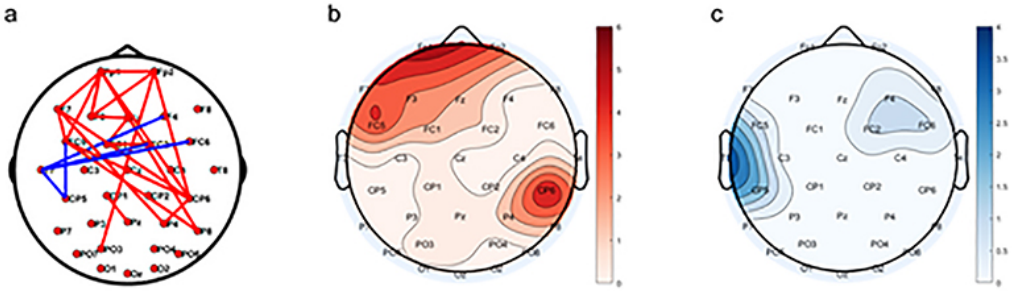

Fig. 2. Differential resting-state network topology pattern in the aspect of the alpha band between the MDD and HC groups. (a) Spatial topology. Red solid lines represent the MDD being greater than that in the HC group, while blue lines indicate the opposite. (b) Degree distribution where the MDD is larger than the HC group. (c) Degree distribution where the MDD is smaller than the HC group.

3. Result

3.1 Baseline Characteristics of the MDD and HC Groups

The Table 1 provides an overview of group demographics and key clinical variables, assessing the comparability of the two groups. For example, it explicitly shows that there were no significant differences in age (t = 0.98, $p = 0.33$) or gender ratio ($\chi^2 = 0.00$, $p = 1.00$) between the groups, while the MDD group had a mean HAMD score of 24.76 ± 3.70, which is significantly higher than that of the HC group (as expected, since HC participants had no depressive symptoms).

3.2 Differential Network Topology Between MDD and HC Group

We then explored the differential resting-state network topologies between MDD group and HC group in the alpha band in Fig. 2a. We found stronger frontal-parietal linkages for the MDD comparison with the HC group in the alpha band ($p < 0.05$, FDR corrected; Fig. 2b,c). There were no significant differences in network properties in terms of the alpha band across the two groups.

3.3 Network Topology Correlated With HAMD in the MDD Group

Fig. 3 presents the significant network topology proven to have a connection with the MDD group's HAMD scores in the alpha band, in which only the long-range frontal-parietal associations of the resting-state network were found to be notably connection with HAMD score ($p < 0.05$. FDR corrected). The stronger frontal-parietal connectivity in the MDD group showed a medium-to-large effect size (Cohen's d = 0.68).

3.4 Relationships Between HAMD Scores and Resting-state Network Properties

We then explored the relationships between HAMD scores and resting-state network properties. As illustrated in Fig. 4, *Clu* ($r = 0.401$, $p = 0.047$), *Ge* ($r = 0.408$, $p = 0.043$), and *Le* ($r = 0.402$, $p = 0.047$) were demonstrated to be significantly positively correlated with HAMD scores, while *Cpl* was negatively correlated with HAMD scores ($r = –0.408$, $p = 0.043$) ($PFDR < 0.05$).

3.5 HAMD Prediction Depending on Resting-state Network Properties

Given that the MDD group showed a strong correlation between the resting-state network properties and HAMD score, resting-state network properties were therefore served as features to predict the HAMD scores in adolescents with depressive symptoms. Fig. 5 presents the scatter plots of the predicted and actual HAMD score ($R^2 = 0.38$, $p < 0.001$), where the *x*- and *y*-axes illustrate the actual and predicted scores, respectively, along with a RMSE

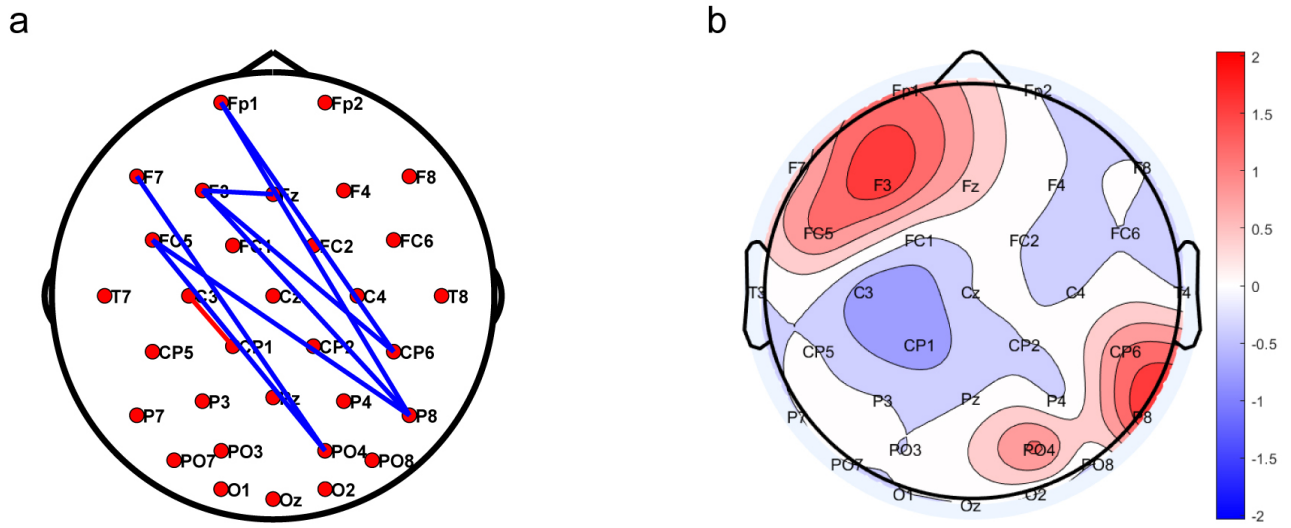

Fig. 3. Network topology correlated with HAMD score in the MDD group. (a) Blue indicates a positive correlation, while red indicates a negative correlation. (b) The frontal-parietal area was found to be activated in the analysis of weighted correlation values in the MDD group.

of 2.8342. The resting-state network properties were eventually utilized to distinguish the two groups, which was also successfully achieved for both the MDD and HC groups, achieving an accuracy of 94%.

4. Discussion

This investigation found substantial differences in resting-state network topology among MDD and HC groups, characterized by heightened activation in frontal-parietal regions and altered global/local connectivity patterns, as evidenced by marked increases in *Clu*, *Ge*, *Le*, and a substantial decrease in *Cpl*. Leveraging the four resting-state brain network metrics as predictive and classification features, a multivariate linear regression model was developed to quantify depression symptom severity, and a binary classification model was constructed to differentiate patient and control cohorts, achieving 94% accuracy. These alterations may reflect a disruption in the optimal topological organization of adolescent brain networks, potentially influencing information processing efficiency—though the precise functional implications remain to be clarified with future studies incorporating source localization.

From the perspective of differential brain network connectivity, the MDD group exhibited abnormal resting-state frontal-parietal topology (see Fig. 2). Some studies found that adolescent patients with depression showed greater right frontal EEG activation and alpha asymmetry during the resting state [37,38]. The activation of the resting-state network and altered connectivity in frontal-parietal regions in adolescent patients may be related to their clinical symptoms [39].

This study identified pronounced correlations between HAMD scores in the MDD group and resting-state network topology (Fig. 3a). Furthermore, analysis of weighted correlations revealed increased activation in frontal-parietal regions within resting-state brain networks in the MDD group (Fig. 3b). At the level of inter-network connections, the significantly enhanced frontal-parietal control network connections compared to healthy individuals may represent some changes in subclinical depression [40–43]. As illustrated in the Fig. 3a, the neural connections traverse distinct brain regions, exhibiting a spectrum of interregional distances, ranging from proximal local linkages to distal long-range pathways. Depression exerts an impact not just on long-range brain connections but also encompasses local neural activity, with symptom severity bearing an inverse relationship to the degree of local activity [44,45].

The results in Fig. 4 suggested that HAMD scores bore a positive relationship with *Clu*, *Ge*, and *Le*, and negatively correlated with *Cpl*. Previous studies have shown that MDD patients display diminished global and local efficiency, which may reflect obstacles in the information processing of the brain network [25,46,47]. The network-based randomized controlled studies suggested that, in comparison with the HC group, MDD patients presented marked network randomization, characterized by longer characteristic path lengths and smaller coefficients of clustering, and reduced global efficiency and local efficiency [47–50]. Unlike previous studies, our research found increased global and local efficiency in the brain networks of the MDD group. It might potentially due to age-related differences (e.g., immature adolescent networks), disorder severity, and EEG frequency band selection [51,52].

To further verify the association between the depression and brain network topology and attributes, a predictive analysis of HAMD scores and a classification task were

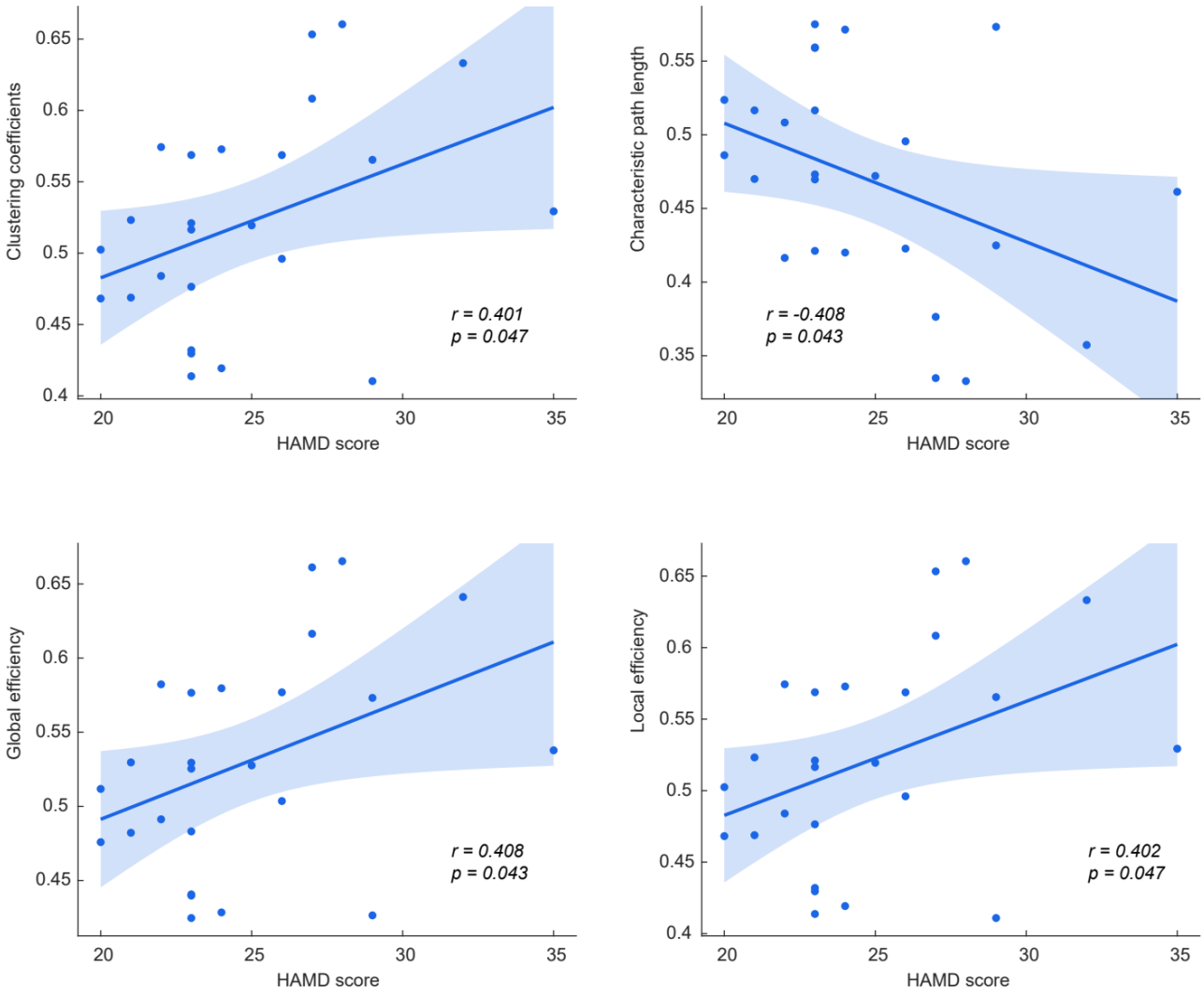

Fig. 4. Relationships between HAMD scores and resting-state network properties of the MDD group.

conducted based on the topology and attributes of resting-state network, which not only predicted the severity of symptoms ($r = 0.637$, $p < 0.05$) but also provided good classification results (an accuracy of 94%) for clinical diagnosis (see Fig. 5). This study found that resting-state network properties can serve as objective biomarkers for predicting the intensity of clinical depressive symptoms in adolescent MDD patients.

Our research results partially accord with the existing literature [53], yet some discrepancies were noted. Our research found increased global and local efficiency in the brain networks of the MDD group. The brain networks of adolescents with MDD demonstrate reduced local segregation alongside increased global integration, reflecting a shift toward a less organized and more homogeneous network configuration [51,52]. Such alterations indicate impaired modular information processing and reduced fault tolerance, which have been shown to correlate with the severity of depressive symptoms. Such findings suggest a disruption in the optimal topological organization of brain networks, potentially influencing the assessment and interpretation of network-based neurophysiological measures [33]. Given the small sample size, our results should be interpreted as exploratory, and future studies with larger cohorts are needed to validate these findings.

A study reveals circuit-level complementarity between frontoparietal alpha-band hyperconnectivity and emotional network dysconnectivity in MDD adolescents, implicating disinhibition in driving pathological connectivity that disrupts emotion-cognition integration [54]. The convergent neuroimaging data from prefrontal-parietal degree centrality and elevated global efficiency establishes frontoparietal dysregulation as a core MDD mechanism, accounting for both the 94% diagnostic accuracy of predictive models and impaired emotion-cognitive processing [55].

Adolescent brain networks undergo a protracted maturation process characterized by refinement of connectivity patterns, with frontal-parietal networks showing delayed development of efficient small-world properties. The increased global efficiency observed in our MDD group may

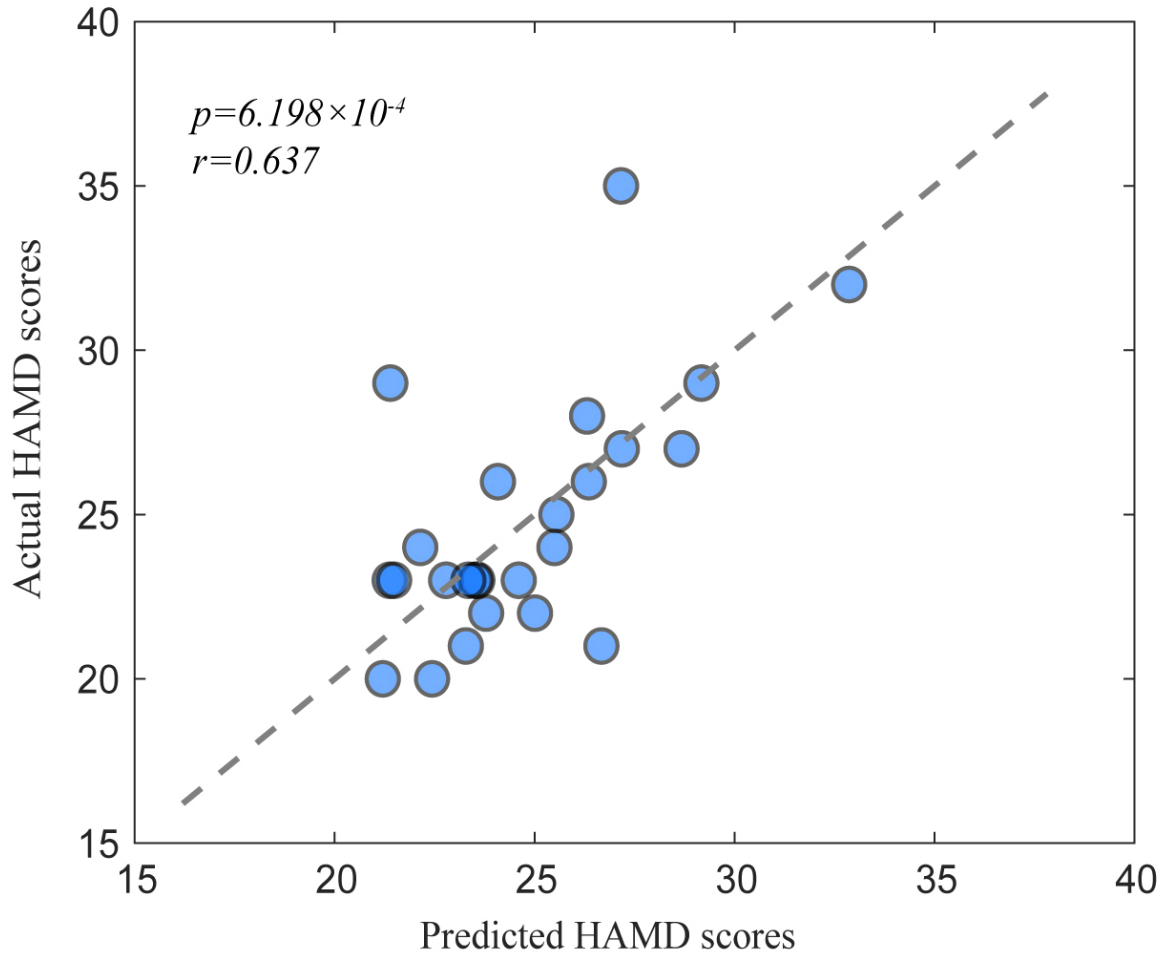

Fig. 5. Predicting HAMD scores based on resting-state brain network.

reflect a disruption of this maturational trajectory, as immature networks often exhibit less specialized connectivity profiles before transitioning to more segregated, adult-like organization.

5. Limitations

One limitation of this study is the quasistationarity assumption for 5-second EEG segments in PLV calculation may overlook transient phase synchronization dynamics. Second, the small sample size potentially limits generalizability and statistical power for detecting subtle effects. Future studies should employ larger, multisite cohorts and time-resolved methods (e.g., sliding-window or time-frequency analyses) to validate the stability of observed network topology patterns and their relationship with HAMD scores.

6. Conclusion

This study demonstrates that frontal-parietal connectivity networks in adolescents with MDD are associated with clinical symptom severity, as indexed by the HAMD. Resting-state EEG network features not only distinguish MDD patients from healthy controls but also predict symptom severity with high accuracy. These findings clarify the neurophysiological features underlying adolescent depression and highlight the translational potential of frontal-parietal connectivity as an objective biomarker for diagnostic refinement and therapeutic monitoring. Further investigations are needed to validate the specificity of these biomarkers and their developmental trajectories in depression progression.

Availability of Data and Materials

The data that support the findings of this study are available upon reasonable request from the corresponding author.

Author Contributions

YK and YS contributed equally as co-first authors. They were responsible for the experimental design, performing the main experiments, data collection and curation, result analysis, and drafting the initial manuscript. LL contributed to the study design and data acquisition. JL participated in experiments and data validation. YZ was in charge

of clinical sample collection and patient data management. WL handled data visualization and figure preparation. JZ participated in the data analysis and interpretation of the results. CW contributed to the study conception, acquired funding, supervised the experimental process, and reviewed and edited the manuscript. HZ was responsible for the overall conceptualization and design of the project, secured the funding, provided overall project supervision and management, and performed the final review and approval of the manuscript. All authors contributed to editorial changes in the manuscript. All authors read and approved the final manuscript. All authors have participated sufficiently in the work and agreed to be accountable for all aspects of the work.

Ethics Approval and Consent to Participate

This study and all experimental protocols were approved by the Institutional Review Board and the Ethics Committee of the Second Affiliated Hospital of Xinxiang Medical University (approval number: XYEFYJSSJ-2023-12). Written informed consent was obtained from all participants and their guardians. This study conformed to the ethical guidelines of the World Medical Association's Declaration of Helsinki.

Acknowledgment

Not applicable.

Funding

This work was supported by the Open Project of the Psychiatry and Neuroscience Discipline of Second Affiliated Hospital of the Xinxiang Medical University (No. XYEFYJSSJ-2023-12), the Project of Science and Technology in Henan Province (No. 242102310363), the Key Scientific Research Projects of Universities and Colleges in Henan Province (No. 242102310074), the National Key Research and Development Program of China (2016YFC1306700 to ZJZ, 2016YFC1306704 to HXZ), the Zhongyuan Talents Program-scientific and technological innovation leading talents (204200510020, to HXZ), Henan Province Joint Construction Project (No. LHGJ20240506), Key Research and Development Projects of Henan Province (241111312800 to WL).

Conflict of Interest

The authors declare no conflict of interest.

References

[1] Sun X, Xia M, He Y. Towards dysfunctional connectome development in depressed adolescents. European Child & Adolescent Psychiatry. 2023; 32: 1147–1149. https://doi.org/10.1007/s00787-023-02223-7.

[2] Okamoto N, Hoshikawa T, Ikenouchi A, Natsuyama T, Fujii R, Igata R, *et al*. Comparison of Serum Metabolomics Pathways and Patterns between Patients with Major Depressive Disorder with and without Type 2 Diabetes Mellitus: An Exploratory Study. Journal of Integrative Neuroscience. 2023; 22: 13. https://doi.org/10.31083/j.jin2201013.

[3] GBD 2019 Diseases and Injuries Collaborators. Global burden of 369 diseases and injuries in 204 countries and territories, 1990-2019: a systematic analysis for the Global Burden of Disease Study 2019. Lancet (London, England). 2020; 396: 1204–1222. https://doi.org/10.1016/S0140-6736(20)30925-9.

[4] Wu B, Chen Y, Long X, Cao Y, Xie H, Wang X, *et al*. Altered single-subject gray matter structural networks in first-episode drug-naïve adolescent major depressive disorder. Psychiatry Research. 2023; 329: 115557. https://doi.org/10.1016/j.psychres.2023.115557.

[5] Wu B, Long X, Cao Y, Xie H, Wang X, Roberts N, *et al*. Abnormal intrinsic brain functional network dynamics in first-episode drug-naïve adolescent major depressive disorder. Psychological Medicine. 2024; 54: 1758–1767. https://doi.org/10.1017/S0033291723003719.

[6] Redlich R, Opel N, Bürger C, Dohm K, Grotegerd D, Förster K, *et al*. The Limbic System in Youth Depression: Brain Structural and Functional Alterations in Adolescent In-patients with Severe Depression. Neuropsychopharmacology: Official Publication of the American College of Neuropsychopharmacology. 2018; 43: 546–554. https://doi.org/10.1038/npp.2017.246.

[7] Schmaal L, Hibar DP, Sämann PG, Hall GB, Baune BT, Jahanshad N, *et al*. Cortical abnormalities in adults and adolescents with major depression based on brain scans from 20 cohorts worldwide in the ENIGMA Major Depressive Disorder Working Group. Molecular Psychiatry. 2017; 22: 900–909. https://doi.org/10.1038/mp.2016.60.

[8] Steingard RJ, Renshaw PF, Yurgelun-Todd D, Appelmans KE, Lyoo IK, Shorrock KL, *et al*. Structural abnormalities in brain magnetic resonance images of depressed children. Journal of the American Academy of Child and Adolescent Psychiatry. 1996; 35: 307–311. https://doi.org/10.1097/00004583-199603000-00011.

[9] LeWinn KZ, Connolly CG, Wu J, Drahos M, Hoeft F, Ho TC, *et al*. White matter correlates of adolescent depression: structural evidence for frontolimbic disconnectivity. Journal of the American Academy of Child and Adolescent Psychiatry. 2014; 53: 899–909.e7. https://doi.org/10.1016/j.jaac.2014.04.021.

[10] van Velzen LS, Kelly S, Isaev D, Aleman A, Aftanas LI, Bauer J, *et al*. White matter disturbances in major depressive disorder: a coordinated analysis across 20 international cohorts in the ENIGMA MDD working group. Molecular Psychiatry. 2020; 25: 1511–1525. https://doi.org/10.1038/s41380-019-0477-2.

[11] Ho TC, Connolly CG, Henje Blom E, LeWinn KZ, Strigo IA, Paulus MP, *et al*. Emotion-Dependent Functional Connectivity of the Default Mode Network in Adolescent Depression. Biological Psychiatry. 2015; 78: 635–646. https://doi.org/10.1016/j.biopsych.2014.09.002.

[12] Cullen KR, Westlund MK, Klimes-Dougan B, Mueller BA, Houri A, Eberly LE, *et al*. Abnormal amygdala resting-state functional connectivity in adolescent depression. JAMA Psychiatry. 2014; 71: 1138–1147. https://doi.org/10.1001/jamapsychiatry.2014.1087.

[13] Qi S, Yang X, Zhao L, Calhoun VD, Perrone-Bizzozero N, Liu S, *et al*. MicroRNA132 associated multimodal neuroimaging patterns in unmedicated major depressive disorder. Brain: a Journal of Neurology. 2018; 141: 916–926. https://doi.org/10.1093/brain/awx366.

[14] Kerestes R, Davey CG, Stephanou K, Whittle S, Harrison BJ. Functional brain imaging studies of youth depression: a systematic review. NeuroImage. Clinical. 2013; 4: 209–231. https://doi.org/10.1016/j.nicl.2013.11.009.

[15] Zhang W, Zhao C, Tang F, Luo W. Automatic Positive and Negative Emotion Regulation in Adolescents with Major De-

pressive Disorder. Psychopathology. 2024; 57: 111–122. https://doi.org/10.1159/000533334.
[16] Zhou P, Wu Q, Zhan L, Guo Z, Wang C, Wang S, *et al*. Alpha peak activity in resting-state EEG is associated with depressive score. Frontiers in Neuroscience. 2023; 17: 1057908. https://doi.org/10.3389/fnins.2023.1057908.
[17] Jiang L, Liang Y, Genon S, He R, Yang Q, Yi C, *et al*. Spatial–rhythmic network as a biomarker of familial risk for psychotic bipolar disorder. Nature Mental Health. 2023; 1: 887–899. https://doi.org/10.1038/s44220-023-00143-8.
[18] Sporns O. Structure and function of complex brain networks. Dialogues in Clinical Neuroscience. 2013; 15: 247–262. https://doi.org/10.31887/DCNS.2013.15.3/osporns.
[19] Kounios J, Fleck JI, Green DL, Payne L, Stevenson JL, Bowden EM, *et al*. The origins of insight in resting-state brain activity. Neuropsychologia. 2008; 46: 281–291. https://doi.org/10.1016/j.neuropsychologia.2007.07.013.
[20] Wu CT, Huang HC, Huang S, Chen IM, Liao SC, Chen CK, *et al*. Resting-State EEG Signal for Major Depressive Disorder Detection: A Systematic Validation on a Large and Diverse Dataset. Biosensors. 2021; 11: 499. https://doi.org/10.3390/bios11120499.
[21] Zhao L, Wang X, Sun G. Positive Classification Advantage of Categorizing Emotional Faces in Patients With Major Depressive Disorder. Frontiers in Psychology. 2022; 13: 734405. https://doi.org/10.3389/fpsyg.2022.734405.
[22] Letkiewicz AM, Funkhouser CJ, Umemoto A, Trivedi E, Sritharan A, Zhang E, *et al*. Neurophysiological responses to emotional faces predict dynamic fluctuations in affect in adolescents. Psychophysiology. 2024; 61: e14476. https://doi.org/10.1111/psyp.14476.
[23] McVoy M, Aebi ME, Loparo K, Lytle S, Morris A, Woods N, *et al*. Resting-State Quantitative Electroencephalography Demonstrates Differential Connectivity in Adolescents with Major Depressive Disorder. Journal of Child and Adolescent Psychopharmacology. 2019; 29: 370–377. https://doi.org/10.1089/cap.2018.0166.
[24] Bohr IJ, Kenny E, Blamire A, O'Brien JT, Thomas AJ, Richardson J, *et al*. Resting-state functional connectivity in late-life depression: higher global connectivity and more long distance connections. Frontiers in Psychiatry. 2012; 3: 116. https://doi.org/10.3389/fpsyt.2012.00116.
[25] Shim M, Im CH, Kim YW, Lee SH. Altered cortical functional network in major depressive disorder: A resting-state electroencephalogram study. NeuroImage. Clinical. 2018; 19: 1000–1007. https://doi.org/10.1016/j.nicl.2018.06.012.
[26] Angelakis E, Lubar JF, Stathopoulou S, Kounios J. Peak alpha frequency: an electroencephalographic measure of cognitive preparedness. Clinical Neurophysiology: Official Journal of the International Federation of Clinical Neurophysiology. 2004; 115: 887–897. https://doi.org/10.1016/j.clinph.2003.11.034.
[27] MO L, GUO T, ZHANG Y, XU F, ZHANG D. The role of ventrolateral prefrontal cortex on emotional regulation of social pain in depressed patients: A TMS study. Acta Psychologica Sinica. 2021; 53: 494. https://doi.org/10.3724/SP.J.1041.2021.00494.
[28] Yi C, Yao R, Song L, Jiang L, Si Y, Li P, *et al*. A Novel Method for Constructing EEG Large-Scale Cortical Dynamical Functional Network Connectivity (dFNC): WTCS. IEEE Transactions on Cybernetics. 2022; 52: 12869–12881. https://doi.org/10.1109/TCYB.2021.3090770.
[29] Wang J, Zuo X, He Y. Graph-based network analysis of resting-state functional MRI. Frontiers in Systems Neuroscience. 2010; 4: 16. https://doi.org/10.3389/fnsys.2010.00016.
[30] Babu Henry Samuel I, Wang C, Hu Z, Ding M. The frequency of alpha oscillations: Task-dependent modulation and its functional significance. NeuroImage. 2018; 183: 897–906. https://doi.org/10.1016/j.neuroimage.2018.08.063.
[31] Latora V, Marchiori M. Efficient behavior of small-world networks. Physical Review Letters. 2001; 87: 198701. https://doi.org/10.1103/PhysRevLett.87.198701.
[32] Zhou Y, Zhu Y, Ye H, Jiang W, Zhang Y, Kong Y, *et al*. Abnormal changes of dynamic topological characteristics in patients with major depressive disorder. Journal of Affective Disorders. 2024; 345: 349–357. https://doi.org/10.1016/j.jad.2023.10.143.
[33] Wu B, Zhang X, Xie H, Wang X, Gong Q, Jia Z. Disrupted Structural Brain Networks and Structural-Functional Decoupling in First-Episode Drug-Naïve Adolescent Major Depressive Disorder. The Journal of Adolescent Health: Official Publication of the Society for Adolescent Medicine. 2024; 74: 941–949. https://doi.org/10.1016/j.jadohealth.2024.01.015.
[34] Si Y, Jiang L, Li P, Chen B, Wan F, Yu J, *et al*. Relationship Between Decision Making and Resting-State EEG in Adolescents With Different Emotional Stabilities. IEEE Transactions on Cognitive and Developmental Systems. 2023; 16: 243–250. https://doi.org/10.1109/TCDS.2023.3263845.
[35] Rubinov M, Sporns O. Complex network measures of brain connectivity: uses and interpretations. NeuroImage. 2010; 52: 1059–1069. https://doi.org/10.1016/j.neuroimage.2009.10.003.
[36] Zhang T, Liu T, Li F, Li M, Liu D, Zhang R, *et al*. Structural and functional correlates of motor imagery BCI performance: Insights from the patterns of fronto-parietal attention network. NeuroImage. 2016; 134: 475–485. https://doi.org/10.1016/j.neuroimage.2016.04.030.
[37] Xie YH, Zhang YM, Fan FF, Song XY, Liu L. Functional role of frontal electroencephalogram alpha asymmetry in the resting state in patients with depression: A review. World Journal of Clinical Cases. 2023; 11: 1903–1917. https://doi.org/10.12998/wjcc.v11.i9.1903.
[38] Sharpley CF, Bitsika V, Shadli SM, Jesulola E, Agnew LL. EEG frontal lobe asymmetry as a function of sex, depression severity, and depression subtype. Behavioural Brain Research. 2023; 443: 114354. https://doi.org/10.1016/j.bbr.2023.114354.
[39] Damborská A, Tomescu MI, Honzírková E, Barteček R, Hořínková J, Fedorová S, *et al*. EEG Resting-State Large-Scale Brain Network Dynamics Are Related to Depressive Symptoms. Frontiers in Psychiatry. 2019; 10: 548. https://doi.org/10.3389/fpsyt.2019.00548.
[40] Yokoyama S, Okamoto Y, Takagaki K, Okada G, Takamura M, Mori A, *et al*. Effects of behavioral activation on default mode network connectivity in subthreshold depression: A preliminary resting-state fMRI study. Journal of Affective Disorders. 2018; 227: 156–163. https://doi.org/10.1016/j.jad.2017.10.021.
[41] Schultz DH, Ito T, Solomyak LI, Chen RH, Mill RD, Anticevic A, *et al*. Global connectivity of the fronto-parietal cognitive control network is related to depression symptoms in the general population. Network Neuroscience (Cambridge, Mass.). 2018; 3: 107–123. https://doi.org/10.1162/netn_a_00056.
[42] Yin S, Li Y, Chen A. Functional coupling between frontoparietal control subnetworks bridges the default and dorsal attention networks. Brain Structure & Function. 2022; 227: 2243–2260. https://doi.org/10.1007/s00429-022-02517-7.
[43] Harding IH, Yücel M, Harrison BJ, Pantelis C, Breakspear M. Effective connectivity within the frontoparietal control network differentiates cognitive control and working memory. NeuroImage. 2015; 106: 144–153. https://doi.org/10.1016/j.neuroimage.2014.11.039.
[44] Yan R, Huang Y, Shi J, Zou H, Wang X, Xia Y, *et al*. Alterations of regional spontaneous neuronal activity and corresponding brain circuits related to non-suicidal self-injury in young adults with major depressive disorder. Journal of Affective Disorders. 2022; 305: 8–18. https://doi.org/10.1016/j.jad.2022.02.040.
[45] Zhao L, Wang D, Xue SW, Tan Z, Wang Y, Lian Z. Aberrant

state-related dynamic amplitude of low-frequency fluctuations of the emotion network in major depressive disorder. Journal of Psychiatric Research. 2021; 133: 23–31. https://doi.org/10.1016/j.jpsychires.2020.12.003.

[46] Yang H, Chen X, Chen ZB, Li L, Li XY, Castellanos FX, *et al*. Disrupted intrinsic functional brain topology in patients with major depressive disorder. Molecular Psychiatry. 2021; 26: 7363–7371. https://doi.org/10.1038/s41380-021-01247-2.

[47] Yan CG, Chen X, Li L, Castellanos FX, Bai TJ, Bo QJ, *et al*. Reduced default mode network functional connectivity in patients with recurrent major depressive disorder. Proceedings of the National Academy of Sciences of the United States of America. 2019; 116: 9078–9083. https://doi.org/10.1073/pnas.1900390116.

[48] Zhang M, Zhou H, Liu L, Feng L, Yang J, Wang G, *et al*. Randomized EEG functional brain networks in major depressive disorders with greater resilience and lower rich-club coefficient. Clinical Neurophysiology: Official Journal of the International Federation of Clinical Neurophysiology. 2018; 129: 743–758. https://doi.org/10.1016/j.clinph.2018.01.017.

[49] Zhao Z, Niu Y, Zhao X, Zhu Y, Shao Z, Wu X, *et al*. EEG microstate in first-episode drug-naive adolescents with depression. Journal of Neural Engineering. 2022; 19: 056016. https://doi.org/10.1088/1741-2552/ac88f6.

[50] Wen Y, Li H, Huang Y, Qiao D, Ren T, Lei L, *et al*. Dynamic network characteristics of adolescents with major depressive disorder: Attention network mediates the association between anhedonia and attentional deficit. Human Brain Mapping. 2023; 44: 5749–5769. https://doi.org/10.1002/hbm.26474.

[51] Long Y, Li X, Cao H, Zhang M, Lu B, Huang Y, *et al*. Common and distinct functional brain network abnormalities in adolescent, early-middle adult, and late adult major depressive disorders. Psychological Medicine. 2024; 54: 582–591. https://doi.org/10.1017/S0033291723002234.

[52] Blank TS, Meyer BM, Wieser MK, Rabl U, Schögl P, Pezawas L. Brain morphometry and connectivity differs between adolescent- and adult-onset major depressive disorder. Depression and Anxiety. 2022; 39: 387–396. https://doi.org/10.1002/da.23254.

[53] Kabbara A, Robert G, Khalil M, Verin M, Benquet P, Hassan M. An electroencephalography connectome predictive model of major depressive disorder severity. Scientific Reports. 2022; 12: 6816. https://doi.org/10.1038/s41598-022-10949-8.

[54] Connolly CG, Wu J, Ho TC, Hoeft F, Wolkowitz O, Eisendrath S, *et al*. Resting-state functional connectivity of subgenual anterior cingulate cortex in depressed adolescents. Biological Psychiatry. 2013; 74: 898–907. https://doi.org/10.1016/j.biopsych.2013.05.036.

[55] Guo X, Wang W, Kang L, Shu C, Bai H, Tu N, *et al*. Abnormal degree centrality in first-episode medication-free adolescent depression at rest: A functional magnetic resonance imaging study and support vector machine analysis. Frontiers in Psychiatry. 2022; 13: 926292. https://doi.org/10.3389/fpsyt.2022.926292.